


Article

Impact Assessment of Digital Elevation Model (DEM) Resolution on Drainage System Extraction and the Evaluation of Mass Movement Hazards in the Upper Catchment

Ahmad Qasim Akbar ^{1,*} , Yasuhiro Mitani ², Ryunosuke Nakanishi ², Ibrahim Djameluddin ³ and Takumi Sugahara ¹

¹ Department of Civil Engineering, Graduate School of Engineering, Kyushu University, Fukuoka 819-0382, Japan; sugahara.takumi.690@s.kyushu-u.ac.jp

² Department of Civil Engineering, Disaster Risk Reduction Research Center, Faculty of Engineering, Kyushu University, Fukuoka 819-0382, Japan; mitani@doc.kyushu-u.ac.jp (Y.M.); r.nakanishi@doc.kyushu-u.ac.jp (R.N.)

³ Faculty of Engineering, Hasanuddin University, Makassar 90245, Indonesia; ibedije@gmail.com

* Correspondence: akbar.ahmad.qasim.279@s.kyushu-u.ac.jp

Abstract: Worldwide, landslides claim many lives each year, with an average of 162.6 deaths reported in Japan from 1945 to 2019. There is growing concern about a potential increase in this number due to climate change. The primary source of shallow and rapid landslides within watersheds is the 0-order basins, which are located above the 1st order drainage system. These active geomorphological locations govern the frequency of mass movement. Despite the recognition of their importance, little attention has been paid to the role of 0-order basins in initiating landslides. Drainage systems can be extracted using the Digital Elevation Model (DEM) in GIS software. However, the effect of DEM resolution on the extraction of 1st order basins remains unexplained. This research develops an algorithm to assess the impact of DEM resolution on the extraction of first-order basins, channel head points, and the identification of approximate 0-order basins. The study includes algorithms to evaluate the correlation between DEM resolution and 1st order drainage system extraction using fuzzy classification techniques for approximate 0-order basins. The algorithm was applied in Toho Village, Fukuoka, Japan, defining the most appropriate DEM and stream definition threshold with an 86.48% accuracy and ± 30 m error margin for channel head points. Critical slip surfaces were identified inside the 0-order basins and validated with a landslide inventory map with a 91% accuracy. The developed algorithms support hazard management and land use planning, providing valuable tools for sustainable development.

Keywords: 1st order drainage system; DEM resolution; drainage system; 0-order basin; landslides; fuzzy classification; hazard management



Citation: Akbar, A.Q.; Mitani, Y.; Nakanishi, R.; Djameluddin, I.; Sugahara, T. Impact Assessment of Digital Elevation Model (DEM) Resolution on Drainage System Extraction and the Evaluation of Mass Movement Hazards in the Upper Catchment. *Geosciences* **2024**, *14*, 223. <https://doi.org/10.3390/geosciences14080223>

Academic Editor: Ioannis Koukouvelas

Received: 4 July 2024

Revised: 3 August 2024

Accepted: 19 August 2024

Published: 21 August 2024



Copyright: © 2024 by the authors. Licensee MDPI, Basel, Switzerland. This article is an open access article distributed under the terms and conditions of the Creative Commons Attribution (CC BY) license (<https://creativecommons.org/licenses/by/4.0/>).

1. Introduction

A sediment disaster or landslide is the downhill movement of soil, rocks, and organic materials under the influence of gravity, resulting in changes to the landform [1]. Heavy rainfall, earthquakes, human activities, and rapid snow melting are recognized as the primary triggering factors for landslides [2–4]. Landslide risk exists in mountainous regions and, every year, causes great life and financial losses [5]. Worldwide, around 300 million people are at risk of slope failure, and about 66 million of those people are living in the areas with a high risk [6]. From 2003 to 2010, the phenomenon resulted in around 70,000 fatalities, and year by year, fatal landslides are increasing [7]. In Japan alone, the data from 1945 to 2019 reveal an average annual fatality rate of approximately 162.6 people [8]. The fatalities vary depending on the maturity level of the nation [8]. However, due to climate change and increases in rainfall, the probability of rapid mass movement is remarkably high, and the number of fatalities may rise in the future.

Landslide disasters are a major problem for society, and to achieve the Sustainable Development Goals (SDGs), a number of researchers have studied the phenomena, and several methodologies have been proposed to mitigate or reduce the risk of landslides. Abraham 2023 [9] researched the similarities between different debris flow locations using field investigations and numerical modeling. The study proposed an integrated methodology to identify the possibility of further debris flows and quantify the similarities between debris flow locations, materials, and geology using field and laboratory investigations and remote sensing data. Youssef 2022 [10] compared a support vector machine (SVM), convolutional neural network (CNN-1 Dimensional), and (CNN-2 Dimensional) landslide susceptibility mapping for the Asir Region, Saudi Arabia. Alcántara-Ayala 2023 [11] researched the physics and modeling of landslides. Abraham 2022 [12] proposed a data-driven approach with a random forest algorithm to estimate the projected area, length, travel distance, and width of landslides using elevation and slope information. The study was applied to the Western Ghats of India. Kavzoglu 2014 [13] used GIS-based multi-criteria decision analysis, support vector machines, and logistic regression for landslide susceptibility mapping in Trabzon province, Turkey. Mallick 2018 [14] used fuzzy-AHP (Analytic Hierarchy Process) multi-criteria decision-making techniques for GIS-based landslide susceptibility evaluation in the Abha Watershed, Saudi Arabia, and others.

In areas with a humid subtropical climate, one of the primary sources of shallow and rapid landslides is located in the watershed, called the 0-order basin. Unchanneled swales or hollows that may occupy sizable areas within upper order drainage basins are referred to as 0-order basins, among other terms. These basins, also known as headwater areas, are typically characterized by geomorphic hollows located in the middle to upper portions of the hillslopes. Gullies and rills exist in the 0-order basin and can carry sediments downslope. However, the physical and conceptual boundaries between gullies and stream channels are fuzzy and still unclear [15]. It is not necessary for a 0-order basin to always have gullies and rills.

0-order basins are crucial locations for the accumulation of water, sediment, and associated geological hazards. They have the potential to transport these materials into streams, often serving as the starting point for debris flows and rapid landslides [16]. This is particularly evident in the sediments that accumulate in the axis of 0-order drainage basins [17–19]. These areas are marked by active geomorphological processes and serve as potential sources of mass movement [20]. 0-order basins have a significant impact on the frequency of landslides that originate from colluvial hollows [19,21] and provide a local depocenter from which hillslope erosion rates can be determined [21]. Additionally, these basins play a crucial role in governing the movement of sediment, water, and nutrients from hillslopes to channel networks [20]. The location of the 0-order basin is closely related to the identification of the 1st order drainage system; however, due to its complexity, the identification of the basin is still a problem.

In the GIS environment, the DEM is commonly used to extract the surface morphology and hydrological modeling. Therefore, several researchers have used the DEM for hydrological modeling. Khyat 2023 [22] used the Shuttle Radar Topography Mission (SRTM) DEM to study the morphometric characteristics of the Hirnayakeshi basin of Maharashtra and Karnataka, India. B. H.P. Maathuis and L. Wang 2006 [23] implemented DEM hydro-processing to extract a drainage system using near-global resolution suitable for hydrological analysis of a larger river basin. J. F. O and D. M. Mark 1984 [24] presented a method to extract drainage networks from gridded elevation data, and the researchers explained that the pattern of drainage was consistent with visual interpretations. Hancock and Evans 2006 [25] studied a channel head's location and its characteristics using the DEM and others.

The resolution and accuracy of DEMs significantly impact hydrological modeling and watershed delineation. High-resolution LiDAR DEMs offer more accurate representations of ground surfaces and hydrological features compared to traditional DEMs derived from

contour maps, which are crucial for modeling surface and subsurface runoff, flow paths, and water movement rates [26].

In Bangladesh, the SWAT model was used to evaluate different DEM sources, resolutions, and area threshold values (ATVs). The findings showed that the best ATV for accurate watershed delineation is about 40 km². Higher-resolution DEMs provided more detailed hydrological features [27]. Furthermore, variations in the vector scales and cell sizes affect the accuracy of simulated watershed hydrographs, with higher-resolution maps leading to better hydrograph simulations, highlighting the importance of appropriate map scales and cell sizes for reliable hydrological predictions [26]. Additionally, a study on surface microtopographic characteristics and hydrologic connectivity using various DEM resolutions found that coarser resolutions eliminate topographic features and reduce depression storage, affecting hydrologic connectivity and surface runoff [28]. Intense work has been carried out on the effect of DEM resolution and its impact on hydrological modeling and morphological feature extraction. However, none of the researchers have proposed a threshold applicable for the extraction of a 1st order basin based on DEM resolution.

On the other hand, researchers are aware of the existence of 0-order basins and the hazards associated with them, but the processes involved in identifying the areas are complex due to geological and morphological factors; therefore, their intricate nature remains a subject of inquiry. Grieve 2018 [29] proposed that the 0-order basin slope and area negatively covary, producing the distinct forms observed between the two physiographic units, which suggested that they arise through competition between spatially variable soil creep and stochastic land sliding. Sidle 2018 [20] studied the 0-order basin as an important link for progress in hydrogeomorphology. However, there are still unanswered questions regarding how the DEM resolution impacts in the extraction of complex drainage systems, especially the 1st order drainage system, and how to identify the 0-order basin for a wide region.

Moreover, in disaster management, researchers strongly emphasize post-disaster scenarios. Less attention has been given to pre-disaster scenarios, which raises an important question: Can future failure surfaces, particularly those within 0-order basins, be accurately simulated before a disaster occurs?

To address these gaps, the purpose of this paper focuses on three main points:

- Assessing the impact of DEM resolution on the identification of 1st order basins and defining thresholds for various DEM resolutions;
- Developing a model to approximate the boundaries of 0-order basins;
- Evaluating the critical slip surfaces within approximate 0-order basins.

On 5 and 6 July 2017, record-breaking heavy rainfall occurred in southern Japan, resulting in widespread slope failures and debris flows in mountainous regions. An algorithm was developed and implemented in Asakura City and Toho Village, Fukuoka Prefecture. Through this study, it has been determined that DEM resolution affects the extraction of the 1st order basin. With a 1 m DEM resolution and stream definition of 0.003 km², 1st order drainage systems can be extracted with an 86.48% accuracy and with a tolerance of a ± 30 m error margin. Moreover, the designed algorithm provides precise and realistic information about the approximate 0-order basin and the critical slip surface considering the morphology of the basin.

The results of this study were validated with the visual interpretation of the landslide after the July 2017 incident, and they show a good match between the actual event and the simulation. In summary, with a 91% success rate in the detection of past landslides, the developed algorithms accurately mapped the 1st order drainage system, channel heads, approximate 0-order basin, and critical slip surface inside a 0-order basin. The generated map will assist the responsible authorities in enhancing disaster mitigation and urban planning in high-risk zones. The anticipated outcomes include the ability to identify risks and assess their severity within 0-order basins.

2. Data Collection

To implement this study, an area of approximately 3256 km² located between Fukuoka, Saga, and Oita Prefectures (Figure 1) was selected.

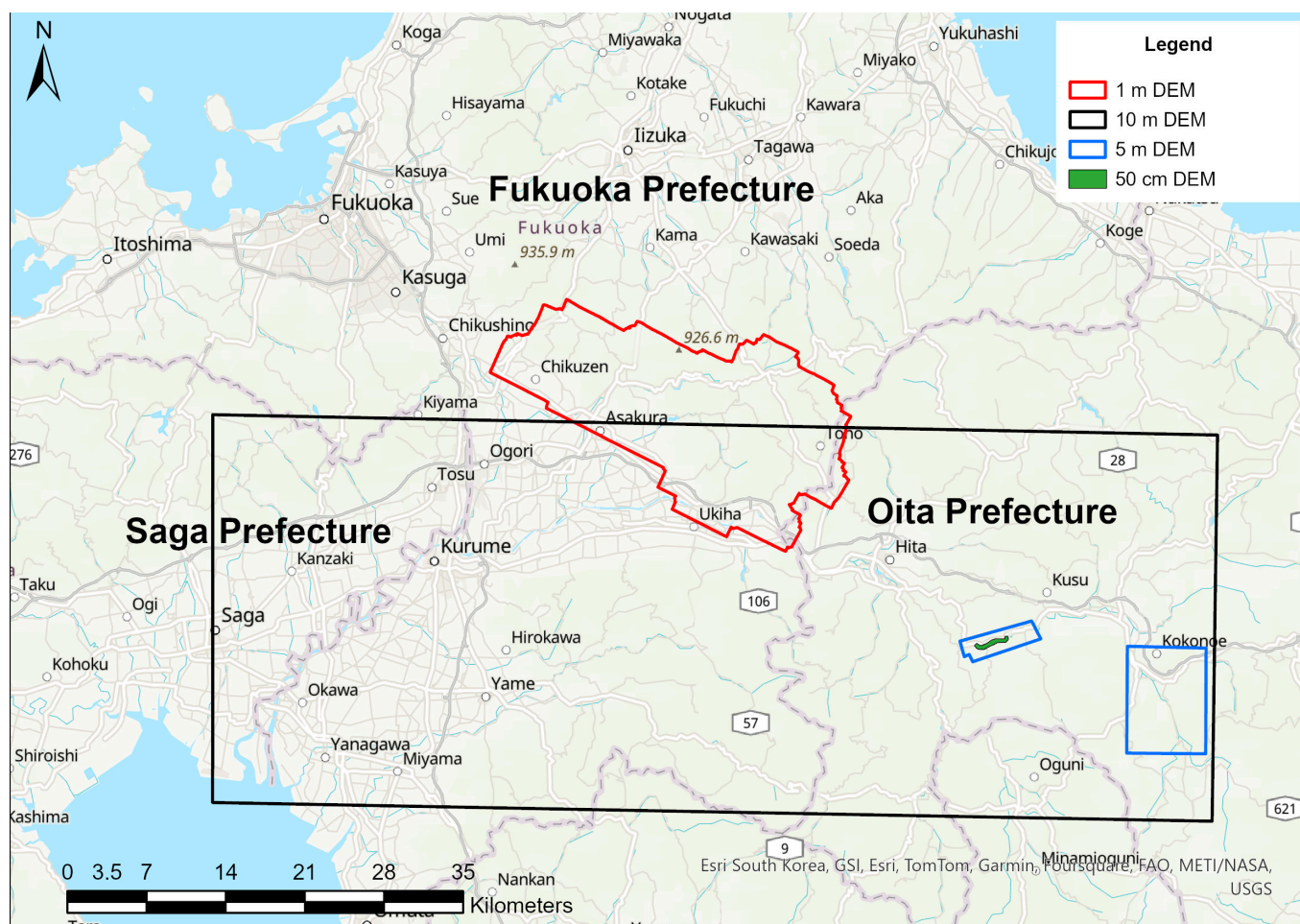


Figure 1. Study area location map.

DEMs with resolutions of 10 m, 5 m, 1 m, and 50 cm were obtained. The DEMs with resolutions of 10 m and 5 m were downloaded from the Geospatial Information Authority of Japan website. The 1 m resolution data were obtained from Asia Air Survey Co., Ltd. Additionally, the 0.5 m existing DEM Laser Profile data were used.

To evaluate the slope stability using 3D Monte Carlo analysis, a lithological/geological map scale of 1:200,000 (Figure 13) from the Geological Survey of Japan is used to select the geotechnical parameters.

3. Methodology

Based on the objective of this research, the methodology is divided into three sections.

3.1. DEM-Based Drainage System Modeling

DEMs are foundational geospatial datasets that are essential for the hydrological and geomorphological studies of a surface. DEM-based drainage system extraction uses DEMs to identify and analyze natural water flow over landscapes [29]. This process is useful in watershed delineation, flood hazard assessment, and environmental planning.

The resolution and accuracy of DEMs are critical for hydrological modeling and watershed delineation. High-resolution LiDAR DEMs provide more precise representations of ground surfaces and hydrological features compared to traditional DEMs [25,27]. This

precision is essential for accurately modeling surface and subsurface runoffs, flow paths, and water movement rates. Additionally, stream threshold values help accurately delineate detailed hydrological features in high-resolution DEMs; the smaller the threshold value, the more detailed the hydrological features [27].

Drainage networks are established by determining flow directions and aggregating the contributing cells on grids computed from DEMs [24,30]. The steepest path that water would take in each grid cell is indicated by the flow direction, and the number of contributing cells to each cell is determined by flow accumulation. Watershed delineation, the next stage in the model, uses flow accumulation grids to trace upstream from selected pour locations and establish watersheds within a study area. Understanding the catchment areas of rivers, streams, and other water bodies requires pinpointing the area that contributes to a given point. By establishing a flow accumulation threshold (stream threshold), stream networks can be identified. A lower threshold value can improve the details of the stream network [27]. Cells with flow accumulation values greater than this limit are considered as part of the stream network. This process identifies stream lengths and their spatial distribution and allows for the classification of streams according to order, facilitating subsequent drainage system studies. DEM-based drainage system extraction has wide-ranging applications, including flood modeling, water resource management, land use planning, and environmental assessments. It is important to know that the topographic depression filling in DEMs affects river drainage patterns and surface runoff. Filling these depressions influences the geomorphic structure of river networks and the hydrologic response of watersheds. Neglecting topographic depressions can significantly alter drainage patterns, water flow paths, and the overall hydrological behavior. Thus, preserving natural depressions in DEMs is crucial for accurate hydrological modeling and reliable flood dynamic and watershed response predictions [31].

Considering the above fact, an algorithm was developed considering the D8 Flow Direction, in which the DEM will be used to fill in missing values and extract the drainage lines and catchment based on the stream threshold values (Figure 2).

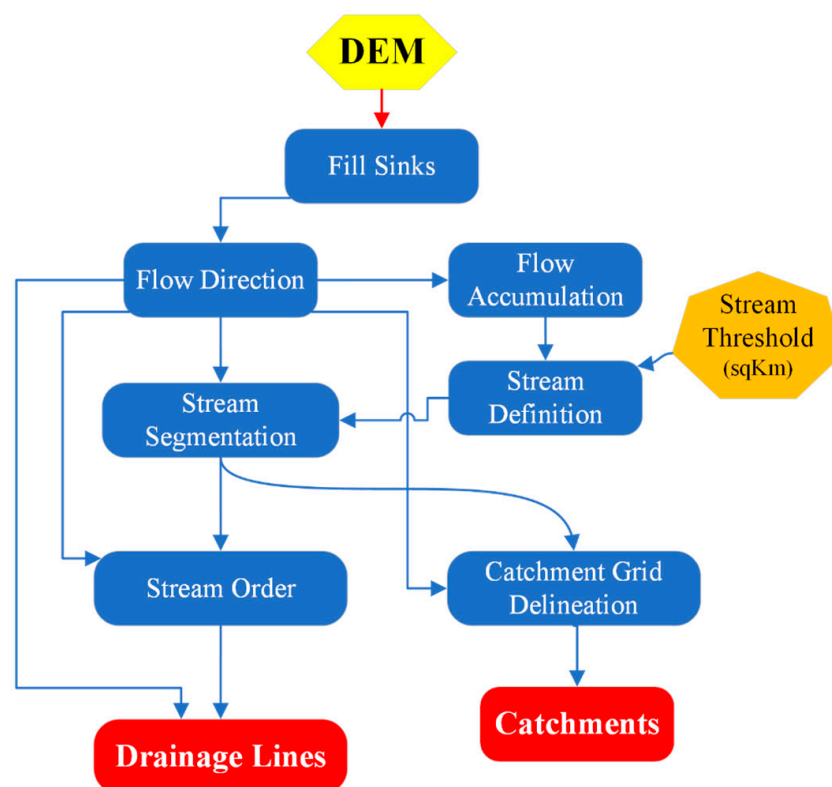


Figure 2. Drainage system algorithm diagram.

3.2. Extraction of Approximate 0-Order Basin

From the explanation of the 0-order basin, it has been clarified that the basin is located in the middle to upper part of the hillslope above the channel head points. In light of this definition, an algorithm was created (Figure 3).

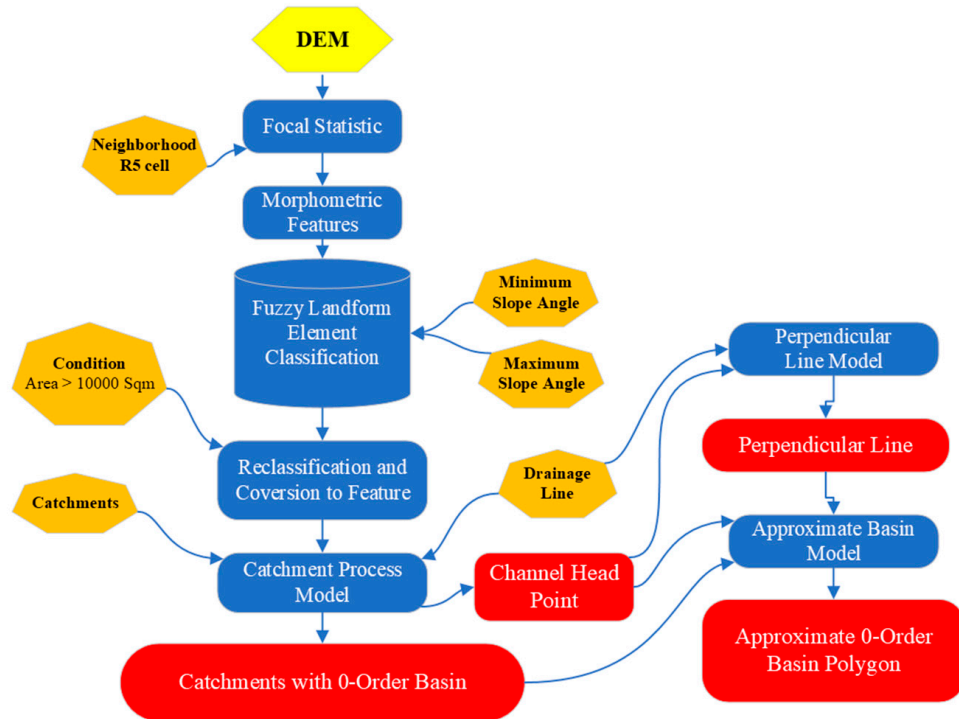


Figure 3. Approximate 0-order basin algorithm diagram.

The fuzzy landform classification algorithm is used to narrow the study’s focus to only 0-order basins. Fuzzy landform classification is an advanced method for categorizing and characterizing landforms using fuzzy logic principles [32]. Unlike traditional classification methods that assign a single category to each terrain feature, fuzzy classification allows for the assignment of multiple categories with varying degrees of membership [33]. This method utilizes the focal statistic to reduce digital DEM noise and extract morphometric layers, which serve as the basis for landform analysis. The focal statistic smooths the DEM data, minimizing artifacts and enhancing the accuracy of subsequent morphometric calculations. Fuzzy logic principles are employed to handle the inherent uncertainty and imprecision in terrain data [34]. In this approach, each landform category is represented by a fuzzy set, and each terrain feature is assigned a membership value (μ) ranging from 0 to 1, indicating the degree to which it belongs to a specific landform category. The membership function $\mu(x)$ can be expressed as:

$$\mu(x) = \frac{1}{1 + e^{-k(x-c)}} \tag{1}$$

In Equation (1), x is the terrain parameter, c is the center of the fuzzy set, and k is the slope parameter controlling the transition between categories. The fuzzy membership values are computed for various terrain parameters, such as slope, curvature, and elevation, and combined to produce a comprehensive landform classification. This methodology offers a flexible and accurate means of portraying and analyzing the intricate and transitional nature of landforms. By assigning membership values to various landform categories, determined by the extent to which a location or terrain feature exhibits the characteristics of each category, fuzzy logic accommodates inherent uncertainty and imprecision [35].

Based on the Nakanishi report [36] on the Otoshi River catchment, the 2017 rain-induced slope failure occurred on slopes between a 28° angle and 37° angle. Therefore, surfaces with angles of 0° to 10° were considered flat, while the rest were categorized as mountainous regions. By using the algorithm, the flat surface was removed, and catchment and channel head points in the mountainous area were extracted. The algorithm allows the user to adjust the value of the flat surface based on their study purpose.

Upon the removal of the flat surface and the channel heads and catchments in the flat surface from the calculation, the algorithm uses the channel head and draws a perpendicular line to the 1st order drainages on the position of the channel head; it is worth mentioning that the direction of a perpendicular line is affected by the shape and direction of the drainage line; therefore, the 1st order drainage line was simplified to reduce the noise generated from the high-resolution DEM. Moreover, the algorithm uses the perpendicular line, channel head drainage line, and mountain catchment and loops the concept (Figure 4) to extrapolate the approximate 0-order basins over a wide region.

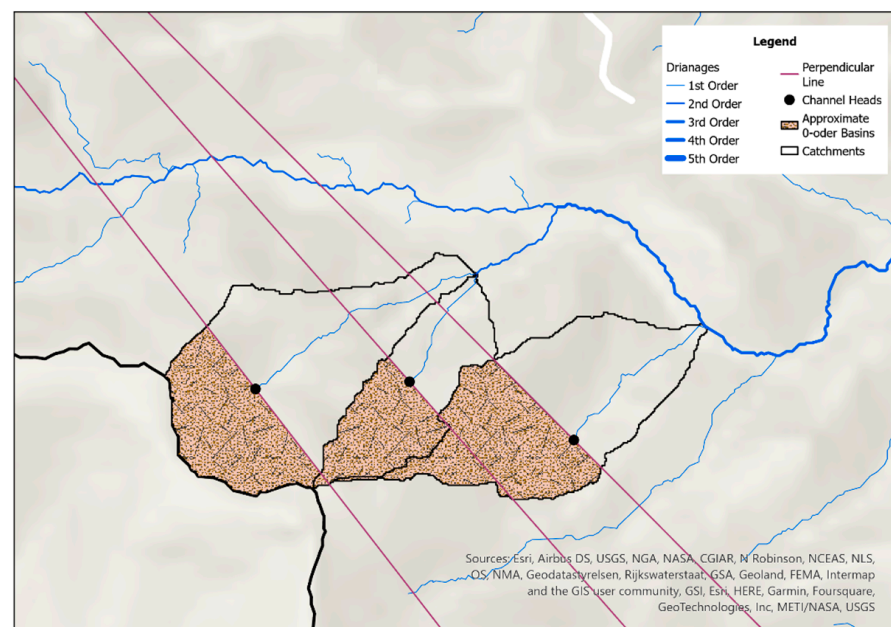


Figure 4. Approximate 0-order basin concept model.

3.3. Critical Slip Surface

The main purpose of defining the approximate 0-order basin in this study is the identification and understanding of rapid mass movement in the 1st order catchments and the identification of high-risk zones within the area [37,38]. Therefore, the evaluation of the critical slip surfaces of the slopes in the approximate 0-order basin is important. The relationship between the slope direction and landslides is fundamental in understanding the complex dynamics of slope instability. The slope direction plays a crucial role in determining the susceptibility of a slope to landslide initiation, with steep slopes facing downhill being more prone to slope failure, particularly during periods of intense rainfall or seismic activity [16].

The gravitational force acting upon a slope, combined with external triggers like heavy rainfall or seismic shaking, can exceed the strength of the slope materials, leading to instability and the initiation of landslides. Once a landslide is triggered, it often follows the path of least resistance, aligning itself with the direction of the slope's descent. The alignment of the slope is critical for guiding the movement of mass downslope along natural pathways, such as channels and gullies, which tend to form along the slope's orientation [39]. As landslides progress downslope, the interaction with the slope's direction continues to shape their dynamics.

Steeper slopes facilitate faster movement velocities, accelerating the mass and increasing the potential for erosion and sediment transport [16]. Moreover, the trajectory of a landslide is influenced by the slope's orientation as it navigates through the landscape, seeking lower-lying areas where the gradient lessens. Lower-lying regions along the path serve as deposition zones, where sediment and debris accumulate as the landslide loses momentum [39]. The deposition process is influenced by the slope's direction, with sediment preferentially settling in areas of reduced movement, such as concave terrain features and valley bottoms.

Beyond the immediate impact of individual landslides, the long-term interaction between the slope direction and landslide dynamics contributes to the landscape's evolution. Repeated landslide events can lead to significant changes in the morphology of the landscape, altering the slope characteristics and reshaping channel networks [40]. The erosion of soil and vegetation from hillslopes, coupled with sediment deposition in valleys and floodplains, influences the overall topography of the area. Understanding this interplay between the slope direction and landslide dynamics is essential for assessing and mitigating the risks associated with these hazardous phenomena.

Hence, for the evaluation of slope stability within the approximate 0-order basin, due consideration is given to the morphology of the slope, and algorithms have been developed (see Figure 5).

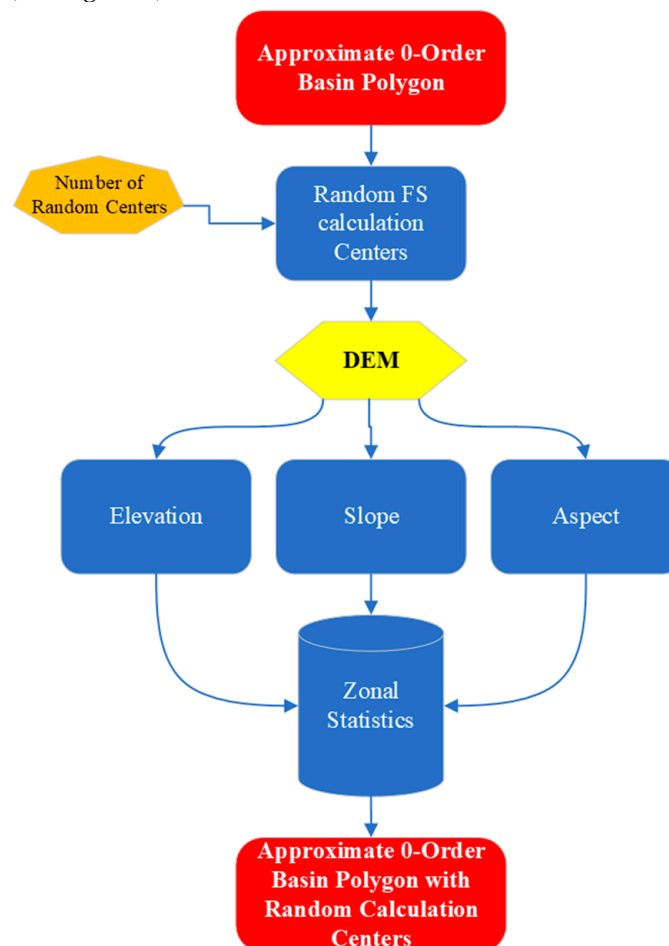


Figure 5. Workflow of random calculation center extraction in approximate 0-order basins.

The algorithm employed utilizes the approximate 0-order basin and generates random calculation centers within its bounds. Following this, zonal statistics are applied to extract the slope, aspect, and elevation information from the DEM in the vicinity of these calculation centers. This algorithm facilitates a deeper understanding of slope characteristics and the direction of slope failure within the 0-order basin (Figure 6).

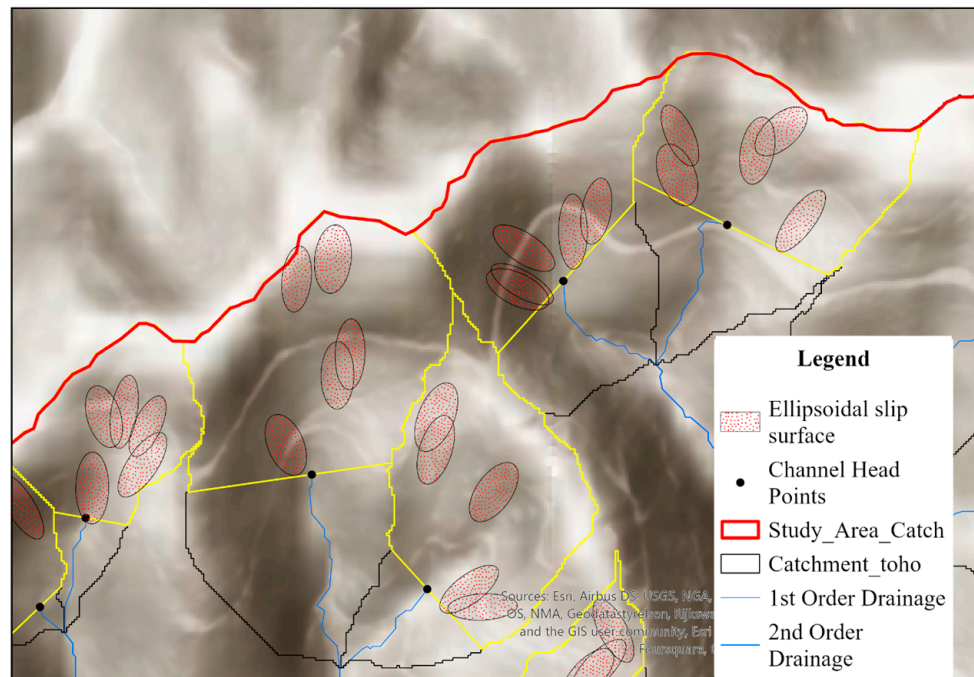


Figure 6. Random calculation center extraction positions inside 0-order basin.

Moreover, to calculate the stability of these slopes, the famous the 3D Monte Carlo approach is used to map the slopes with the highest probability of failure. The Monte Carlo approach is a popular method for slope stability risk analysis among civil engineers. This technique is a probabilistic method used to assess slope stability, involving the generation of several random scenarios for the slope and calculating the factor of safety for each scenario [41]. It uses 3D limit equilibrium methods for slope stability analysis (Equation (2)).

$$FS_{3D} = \frac{\sum_J \sum_i [c' A + (W \cos \theta) \tan \phi'] \cos \theta_{Avr}}{\sum_J W \sin \theta_{Avr} \cos \theta_{Avr}} \quad (2)$$

A is the area of the slip surface; θ is the slope angle of the slip surface; θ_{Avr} is the apparent dip in the main inclination direction of the sliding mass; W is the weight of the soil column; ϕ' is the effective friction angle; c' is the effective cohesion. The shape of the slip surface is considered as ellipsoidal as Figure 7.

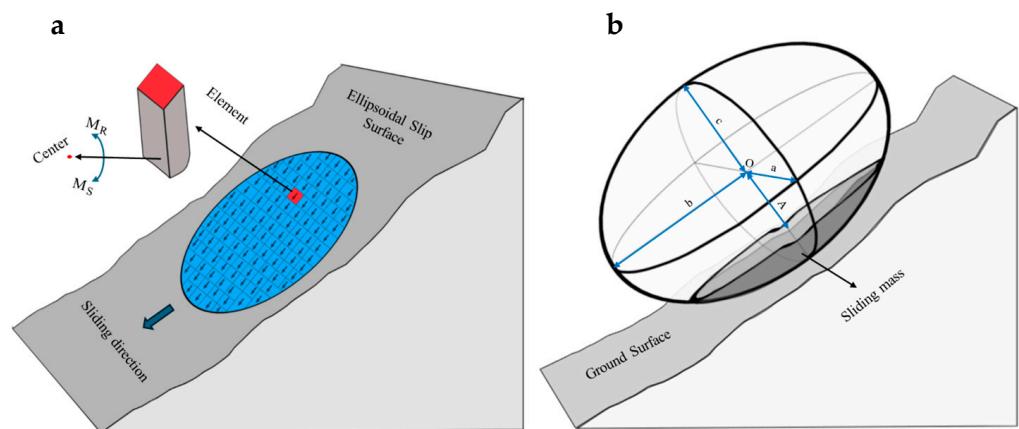


Figure 7. (a) Diagram of an ellipsoidal slip surface showing the sliding direction, center, and elements. (b) Representation of the sliding mass along the ellipsoidal slip surface, with the ground surface and the axes.

An ArcGIS-based tool was developed by Cheng Qiu in 2006 [42] to assess the 3D spatiotemporal characteristics of landslide hazards. The limitation of the tool in considering the slope geology and morphology was improved in the algorithms designed. The improved diagram of the software is as follows, in Figure 8.

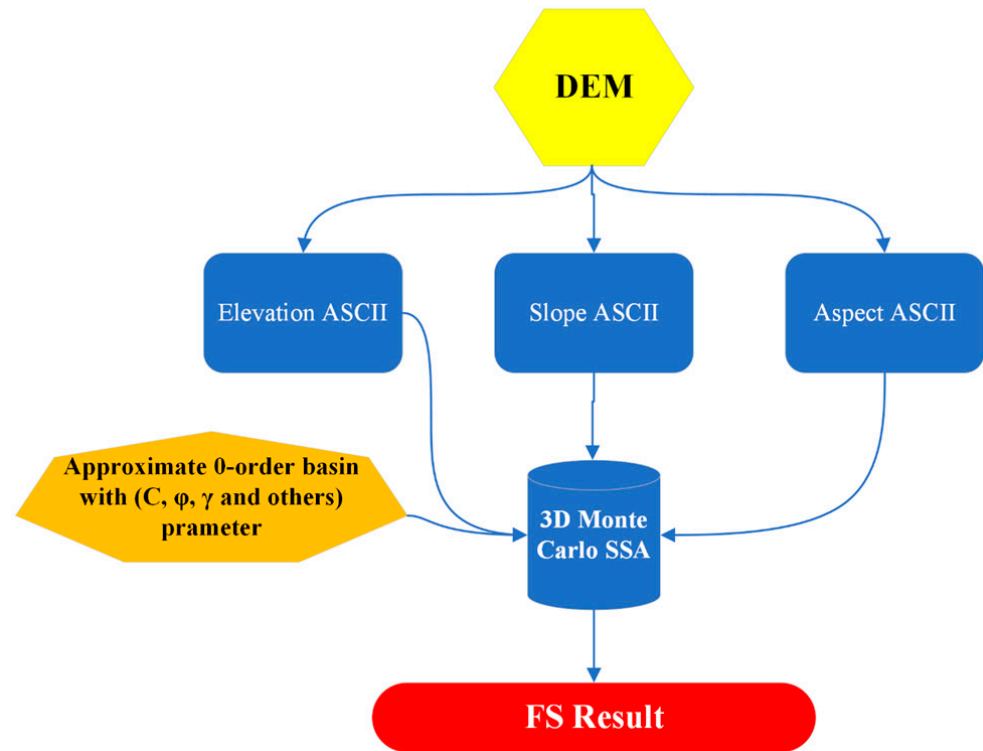


Figure 8. 3D Monte Carlo slope stability analysis.

The modified software will aid in the accurate calculation of the critical surface inside approximate 0-order basins considering the geology and morphology or the slope.

4. Results

4.1. DEM-Based Drainage System Modeling

The study was applied to a wide region of approximately 3256 km² located between Fukuoka, Saga, and Oita Prefectures (Figure 1) to investigate the relationship between DEM resolution and the extraction of 1st order drainage systems (Table 1).

Table 1. Results of DEM resolution influence in drainage systems.

Drainage System	10 m DEM	5 m DEM	1 m DEM	50 cm DEM
6 th order drainage system	Best result			
5 th order drainage system				
4 th order drainage system (>0.3 km ²)	Best result			
3 rd order drainage system (0.3 km ²)	Acceptable	Best result		
2 nd order drainage system (0.017–0.012 km ²)	Noise	Acceptable	Best result	
1 st order drainage system (0.003–0.002 km ²)	Noise		Best result	
Runnels (<0.002 km ²)	Noise		Acceptable	Best result
Smaller runnels	Noise		Noise	

In the table, the “Best result” category in green shows the drainage systems with the closest pattern to the surface morphology. The “Acceptable” category in yellow indicates that the drainage system generally follows the surface morphology; however, on some low-slope-angle surfaces, it generates several unnecessary branches. The “Noise” category in orange, occurs when the drainage system follows the drainage pattern in such detail that it becomes hard to distinguish, leading to the generation of several branches on flat surfaces, which can cause confusion.

The results obtained using the algorithm indicate that the resolution of the DEM plays a crucial role in the detection of stream orders. As depicted in Table 1, a 10 m DEM resolution allows for the extraction of a 3rd order drainage system, whereas with a 5 m DEM, a 2nd order drainage system can be identified. In the case of a 1 m resolution DEM with a threshold of 0.003 to 0.002, the detection of a 1st order drainage system differs from case to case. Conversely, using a 50 cm LP DEM provides highly detailed information on the surface. Not only can the 1st order basin be identified, but also, small surface runnels (gullies and rills) can be extracted. It is important to note that for regional studies, the inclusion of these small surface runnels is not necessary and can lead to confusion.

The location of the 0-order basin is closely tied to the channel head and the reach of 1st order drainage. On the other hand, large-scale mapping of the drainage system in the study area is yet to be undertaken. Therefore, as shown in Figure 9, the validation point is strategically placed where the aspect indicates a consistent direction, and there is a scarcity on the land surface caused by the drainage.

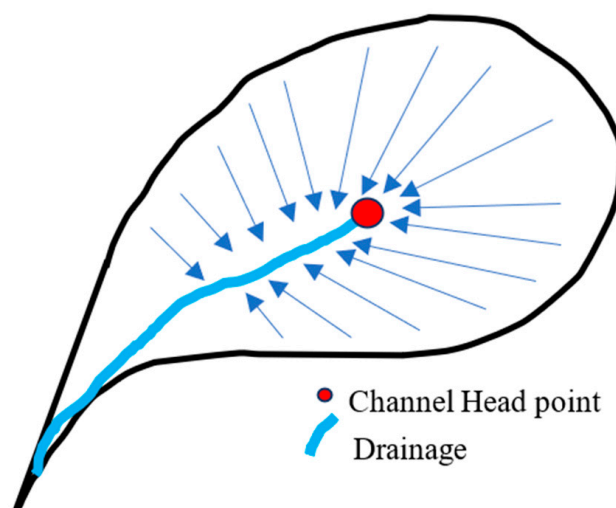


Figure 9. Schematic of drainage system.

This mapping effort aims to reveal the spatial dynamics and hydrological characteristics of the area. The ongoing systematic mapping process promises a clearer understanding of the drainage network, facilitating informed assessments of the region’s hydrological dynamics and validation and error margins of the developed algorithm. Based on the assumption, a total of 392 channel head points were visually drawn from a 1 m DEM and the aspect direction (Figure 10).

Figure 10 shows the locations of channel head points, illustrating that they are influenced not only by topographic depressions caused by the fill sink algorithm in the DEM but also by the stream definition threshold. Therefore, several buffer zones with different distances (± 5 m, ± 10 m, ± 30 m, ± 40 m, and ± 50 m) were drawn around the validation points. These validation points, extracted from the visual interpretation in Figure 9, were used to validate the output obtained from the developed algorithm in the study area. This approach ensures a robust validation process, aligning with the systematic mapping efforts and contributing to the overall understanding of hydrological dynamics.

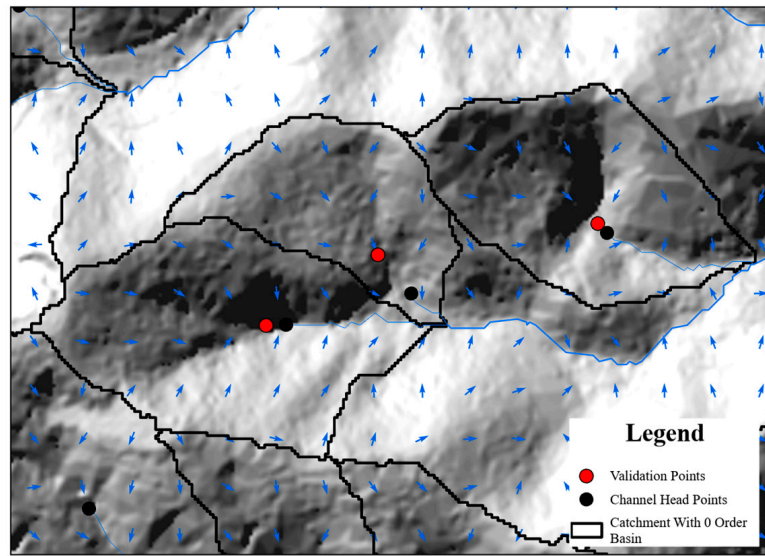


Figure 10. Visual interpretation of channel head points.

The number of channel head points in each buffer zone was compared with the total number of channel points in the study area. The results were calculated considering Equation (3).

$$Result\ in\ \% = \frac{CHB}{TCH} \times 100 \tag{3}$$

In Equation (3), *CHB* is the number of channel head points inside the buffer zone, and *TCH* is the total number of channel heads.

As shown in Figure 11, it can be observed that the algorithm has an acceptable error margin of ±30 m for regional-scale studies; with the mentioned error margin, the algorithm would have an 84.48% accuracy; however, for large-scale studies, it would be beneficial to conduct site investigations.

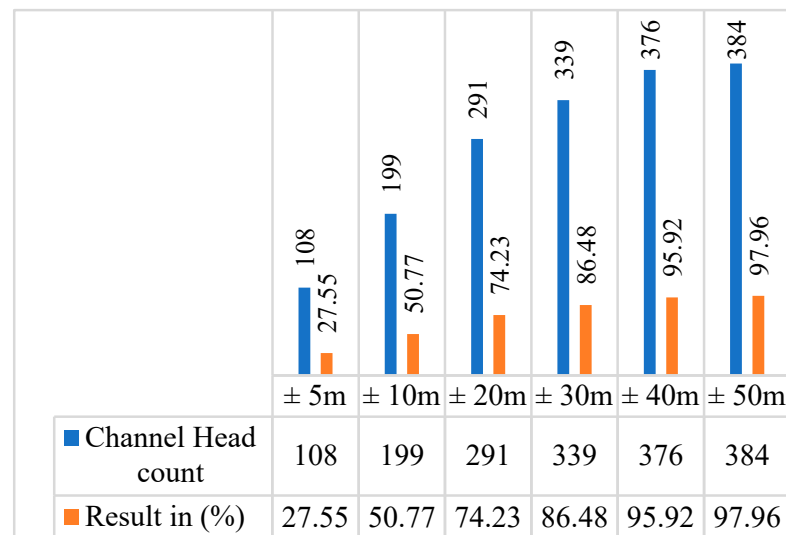


Figure 11. Results of the algorithm.

Additionally, the validation results indicate that the effect of the fill sink algorithm on topographic depressions in the high-resolution DEM is minimal. The locations of channel head points were accurately identified, and the overall impact on drainage patterns and hydrological behavior was insignificant; the use of the fill sink algorithm produces acceptable results for this study.

4.2. Extraction of Approximate 0-Order Basin

After establishing specific thresholds for each DEM type, the algorithm was implemented within Asakura City, a region perpetually afflicted by geo-disasters. A contiguous area spanning 365.29 km², utilizing a 1 m resolution DEM, was chosen for the study. Subsequently, the algorithm was employed, yielding the extraction of 1st order drainages, an impressive count of 27,000 catchments, the identification of channel heads, and the determination of approximate 0-order basins within the designated area (Figure 12).

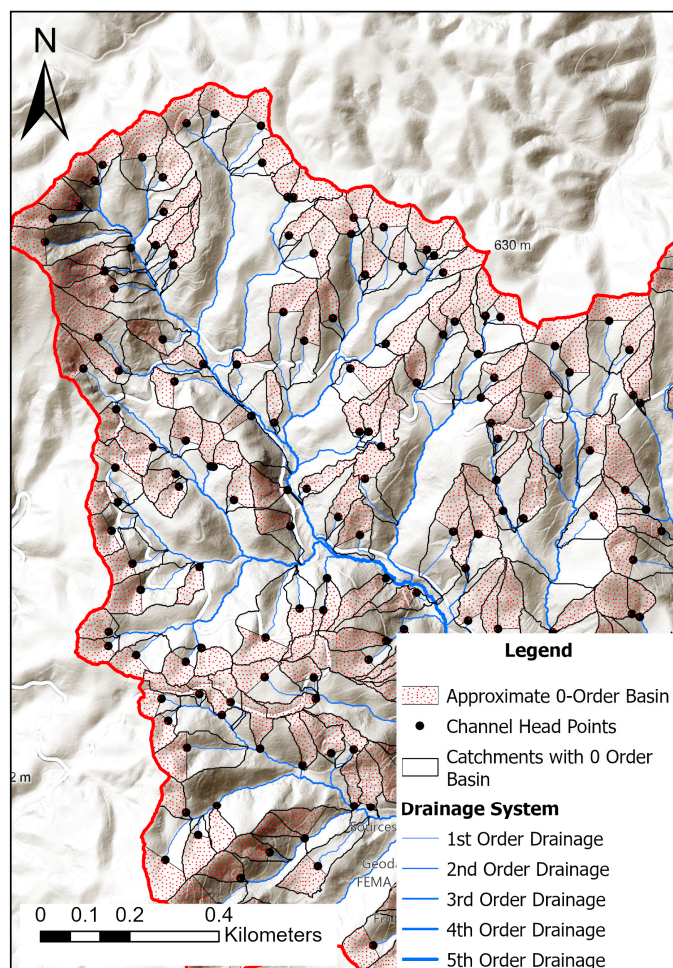


Figure 12. Otoishi River catchment drainage system and approximate 0-order basin.

The results reveal that the algorithm effectively eliminated catchments located in flat areas and catchments with no 1st order drainage system. Moreover, leveraging the principles of the 0-order basin concept, the algorithm primarily relied on channel heads, 1st order drainage, and catchments to extract the approximate 0-order basins in the catchment. In summary, the algorithm's outcomes satisfactorily address the research objective and align with the study's overarching aim by identifying the approximate 0-order basins.

4.3. Critical Slip Surface

To delineate the critical slip surface, the focus was concentrated on the Otoishi River catchment. This specific area comprises a notable 447 channel heads and approximate 0-order basins. Geological analysis was conducted using the 1:200,000 scale geological map provided by the Geological Survey of Japan, revealing that the region is characterized by various geological formations. These formations encompass volcanic rocks such as andesite, basaltic andesite, and granodiorite, as well as medium-grade metamorphic rocks like schist, and sedimentary rocks including breccia, altered sandstone, and mudstone (Figure 13).

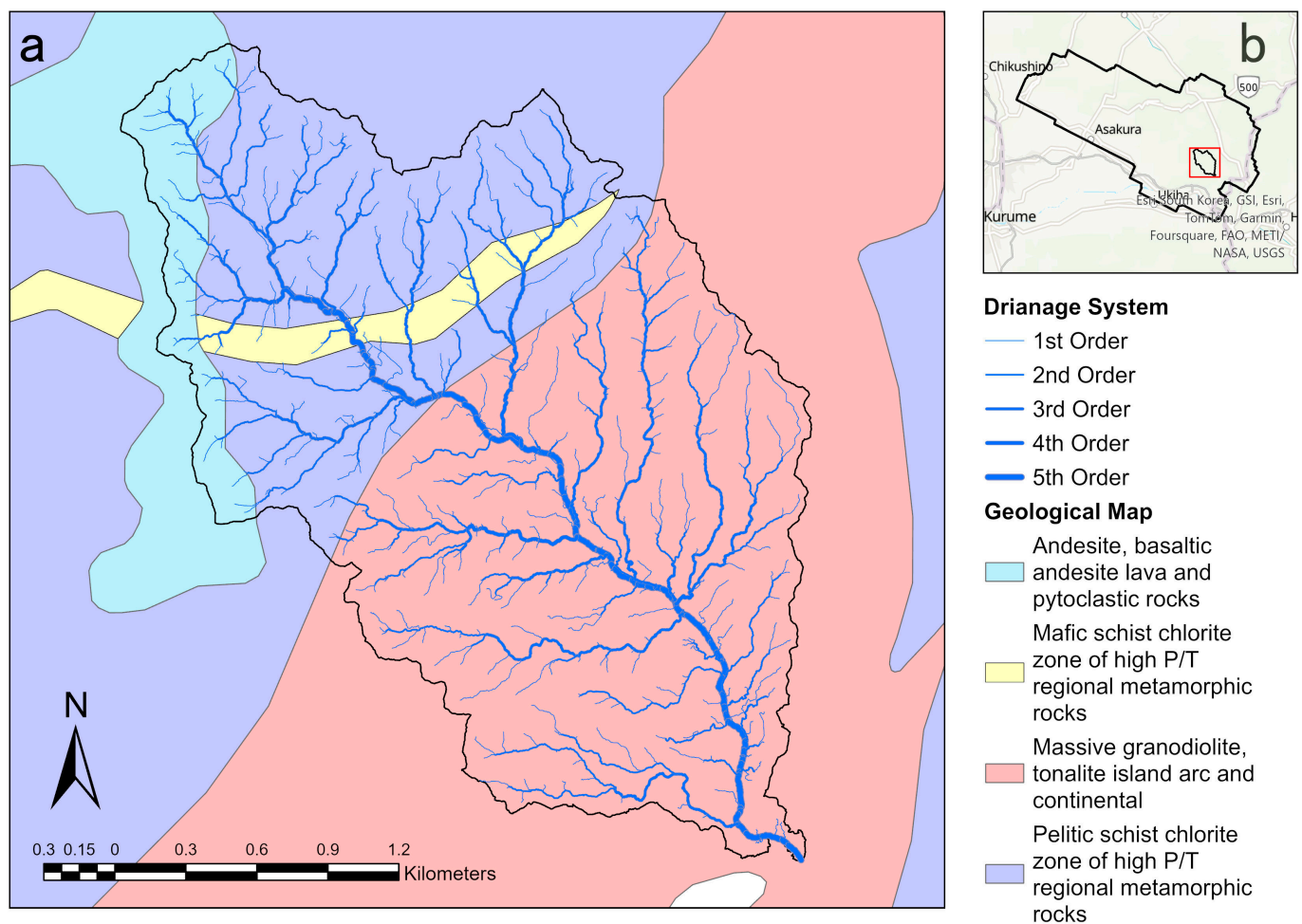


Figure 13. (a) 1:200,000 scale geological map of the Otoishi River catchment. (b) Location map of the study area with an overview of the surrounding cities.

To simulate the critical conditions and execute the 3D MC calculation, an understanding of the geotechnical parameters is needed. The selection of geotechnical parameters for this study was based on a thorough onsite investigation conducted in the Shiraki Valley River. The investigation, which was carried out on igneous rocks in the weathered granitic amphibolite sediments, revealed cohesion values ranging from 12 to 16 kN/m² and internal friction angles ranging between 25° and 30°. The metamorphic rock parameters were selected based on geotechnical studies conducted on the weathered metamorphic rocks by researchers [42–45]. To simulate the critical condition for the slopes, the following parameters were selected for this study (Table 2):

Table 2. Geotechnical parameters of sediments in the study area for MC calculation.

Sediment Type	Cohesion	Fraction Angle	Rock Density
Igneous rocks (andesite, basaltic andesite, and granodiorite)	12 $\frac{\text{kN}}{\text{m}^2}$	25°	24 $\frac{\text{kN}}{\text{m}^3}$
Metamorphic rocks (schist) and sedimentary rocks (breccia)	5 $\frac{\text{kN}}{\text{m}^2}$	20°	20 $\frac{\text{kN}}{\text{m}^3}$

Utilizing these parameters, the algorithm adeptly conducted simulations to calculate the factor of safety for the slip surface within the approximate 0-order basin. The resulting factor of safety values was categorized into five distinct classes, ranging from “very high”, in red, to “very low”, in green (Figure 14).

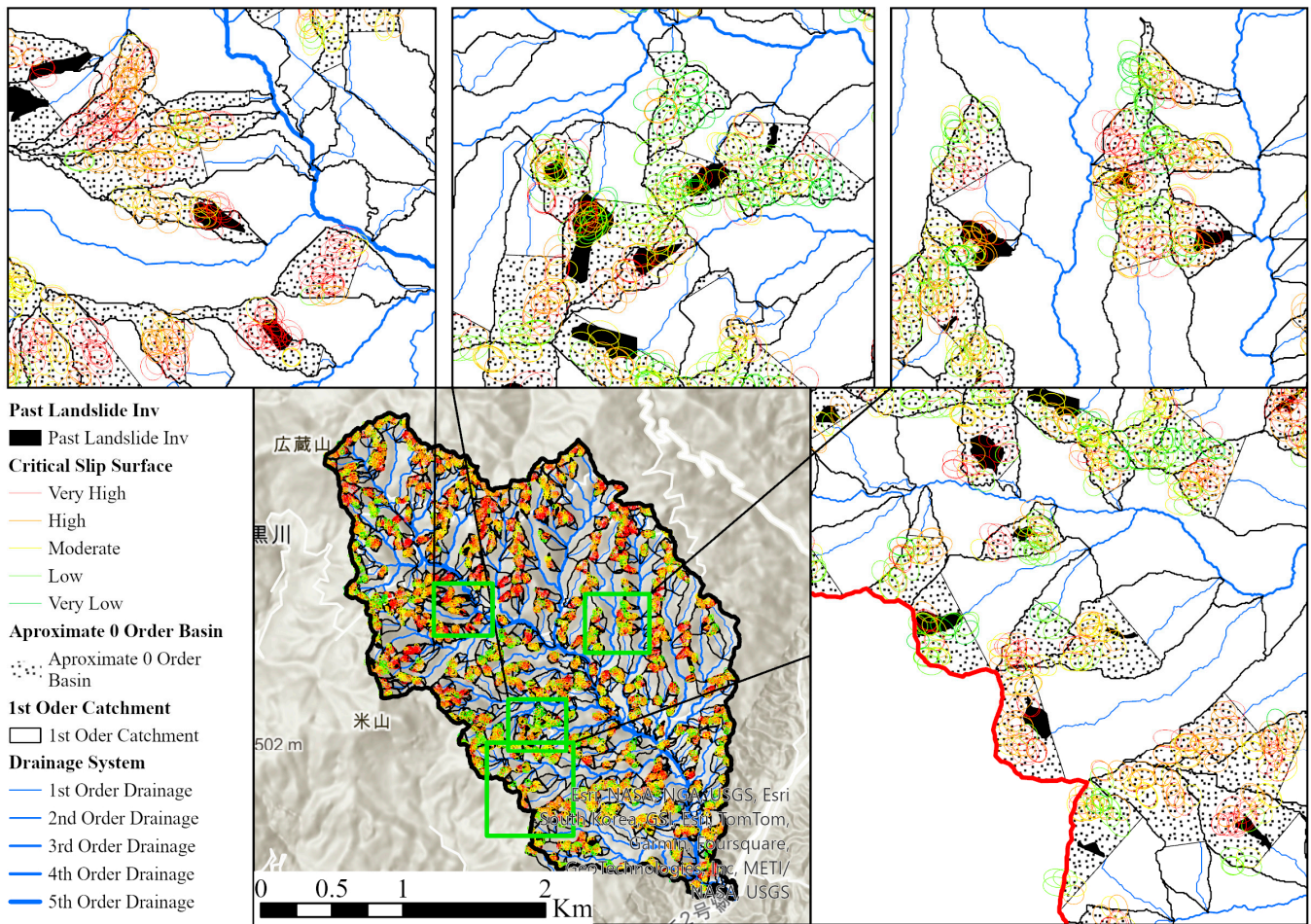


Figure 14. Results of critical slip surface calculation.

Where very high zones are areas with FS values below 1, FS values between 1 and 1.2 are classified as high, FS values between 1.2 and 1.5 are considered moderate, FS values between 1.5 and 3 are categorized as low, and FS values above 3 are categorized as very low.

The result was validated with the visual interpretation of landslide inventory maps after the July 2017 incident. The black polygons shown in Figure 14 correspond to the outcomes of visually interpreting slope failures following the mass movements in the Toho area. It can be inferred that the newly adapted 3D Monte Carlo (MC) algorithm performs admirably in accurately identifying the slip surface within the approximate 0-order basin. The calculation shows that out of 95 recorded landslides after the July 2017 incident, 87 of them were detected using the improved algorithm, representing a 91% accuracy rate. Additionally, new possibilities with the FS below and equal to 1.2 have been identified, which should be considered high-risk zones. It is important to mention that visual interpretation, especially in areas densely covered by vegetation, could have some margin of error. Moreover, during the visual interpretation process, the source of the mass movement was not factored into consideration; however, the algorithm overcomes the limitations and provides information about the potential source of critical slip surface.

5. Discussion

This study provides compelling evidence that DEM resolution is crucial for accurately extracting drainage systems and identifying 0-order basins, which are essential for effective landslide hazard assessment and mitigation. Utilizing high-resolution DEMs (1 m and 50 cm) significantly enhances the precision of drainage network modeling, though each resolution has its own set of advantages and limitations. The resolution of DEMs plays

a significant role in hydrological modeling and watershed delineation. Coarser DEM resolutions tend to eliminate topographic features and reduce depression storage, affecting hydrologic connectivity and surface runoff [28]. High-resolution LiDAR DEMs provide more precise ground surface representations compared to traditional DEMs derived from contour maps. This precision is crucial for accurately modeling surface and subsurface runoff, flow paths, and water movement rates, as demonstrated in various studies [26–28].

Physical-based methods for drainage system extraction, grounded in fundamental hydrological principles and detailed environmental simulations, offer an alternative to traditional techniques by directly modeling complex interactions between water and terrain [46]. However, these methods are resource intensive, requiring significant computational power and high-quality input data, which can limit their practical applicability, particularly for large-scale or real-time applications [47,48]. In contrast, traditional DEM-based methods, while sometimes relying on arbitrary thresholds to define river networks, are more efficient and accessible, making them suitable for large-scale drainage pattern analysis and watershed management. Advances in DEM resolution and processing techniques have enhanced the accuracy and reliability of these methods, ensuring they remain a practical and robust choice for hydrological studies [47]. Combining the strengths of both approaches can lead to more comprehensive and effective drainage pattern analysis strategies.

Higher-resolution DEMs, such as the 1 m and 50 cm models, offer detailed and accurate representations of drainage networks. The 1 m DEM, with an accuracy of 86.48% and an error margin of ± 30 m for channel head points, has proven suitable for extracting 1st order drainage systems. However, the 50 cm DEM, while more detailed, captures smaller features such as gullies and rills, which may not be necessary for regional studies and could introduce noise, leading to potential confusion during interpretation. This suggests that while high-resolution DEMs are beneficial, the choice of resolution must be aligned with the specific objectives of the study to avoid overcomplication.

The development of an algorithm to approximate 0-order basins represents a significant advancement in understanding sediment accumulation and potential landslide initiation areas. 0-order basins, located above 1st order drainages, are critical zones for water, sediment, and associated geological hazards. These basins, often found in the middle to upper parts of hillslopes, serve as starting points for debris flows and rapid landslides due to their active geomorphological processes. The algorithm effectively excluded catchments in flat areas and those without 1st order drainage, focusing on mountainous regions. It demonstrated high efficacy in approximating 0-order basins by leveraging channel heads, 1st order drainage, and catchments. This approach aligns with the geomorphological principles highlighted by Grieve [29] and Sidle [20], who emphasized the importance of 0-order basins in hydrogeomorphology.

On the other hand, after defining the approximate 0-order basins, evaluating critical slip surfaces within these basins is essential for understanding rapid mass movements and identifying high-risk zones. The study employed a 3D Monte Carlo simulation approach, a probabilistic method widely used in civil engineering for slope stability assessment. This approach involves generating multiple random scenarios for slope failure using geotechnical parameters. Slope morphology and geotechnical parameters are pivotal in determining the stability of slopes within 0-order basins. Understanding geotechnical parameters is crucial, as they directly influence the factor of safety calculations, which indicate the likelihood of slope failure.

The 3D Monte Carlo simulation approach used in this study allows for a comprehensive assessment of slope stability by considering various potential failure scenarios. The algorithm achieved a 91% accuracy rate in detecting past landslides, validated against the 2017 landslide inventory in Toho Village, Japan. This accuracy underscores the algorithm's potential for pre-disaster planning and hazard management, enabling authorities to map high-risk zones and inform urban planning and infrastructure development to mitigate potential landslide hazards.

The integration of the Monte Carlo simulation approach with GIS tools enhances the practicality and applicability of the algorithm. GIS-based tools allow for the spatial analysis and visualization of high-risk zones, making it easier for decision makers to interpret and utilize the data. This integration is crucial for effective disaster hazard management, as it provides a clear and accessible representation of landslide-prone areas.

6. Conclusions

After assessing the impact of DEM resolution on drainage system detection, significant distinctions were found. Using a 10 m DEM, 3rd order drainage systems were discernible. With a 5 m DEM, 2nd order drainage systems became identifiable. Employing a 50 cm DEM allowed for the detection of 1st order drainage systems and smaller runnels, such as gullies and rills, which are the main sources of mass movement in the upper drainage system. However, since the boundaries of 1st order basins and gullies/rills are often not clearly defined, this generates confusion, and 50 cm DEMs are economically unsuitable for regional studies; thus, this study does not recommend them. Considering the ± 30 m error margin and 86.48% accuracy, it can be concluded that a 1 m DEM is a suitable resolution for extracting 1st order drainage systems.

Moreover, the newly developed algorithm proves highly effective in delivering precise results for approximately 0-order basins. It includes accurate calculations and the identification of critical slip surfaces or sources of shallow landslides within these basins, signifying high-risk zones based on the geology of the sediments and basin morphology. The verification of the results through virtual interpretations of actual disasters revealed limitations in the omission of mass movement sources and extension due to vegetation cover. The algorithm simulates realistic scenarios with a 91% accuracy rate in detecting past mass movements in 0-order basins, providing information on sliding sources and severity. The generated map is expected to bolster disaster mitigation and urban planning in high-risk zones, assisting in hazard identification within 0-order basins.

Overall, this study underscores the importance of DEM resolution in geomorphological feature extraction and landslide hazard assessment. Integrating high-resolution DEMs with advanced algorithms enhances the precision of drainage system modeling and 0-order basin identification. These advancements significantly contribute to geomorphology and provide practical tools for hazard management and urban planning, ultimately supporting the creation of safer and more resilient communities. Future research should continue exploring the balance between DEM resolution and practical applicability to ensure that the tools developed remain accurate and manageable for diverse applications.

Author Contributions: A.Q.A., R.N., I.D. and T.S. made significant contributions to various aspects of the research, including conceptualization, methodology, algorithm development, data collection, writing the original draft, visualization, and conducting the research. Y.M. was responsible for supervision, conceptualization, methodology development, investigation, review, and editing. All authors have read and agreed to the published version of the manuscript.

Funding: This research was supported by the JST SPRING, Japan, grant number JPMJSP2136.

Data Availability Statement: Since this research aims to provide useful insights into disaster prevention and assist authorities and researchers in achieving the SDGs, the algorithms developed in this study will be made available as a package to authorities and researchers working for humanitarian and educational purposes upon request. The corresponding author is obligated to make the datasets and algorithms used in this research available.

Acknowledgments: The authors sincerely thank the JST SPRING, Japan; Council for Science, Technology and Innovation (CSTI) of the Cabinet Office, Government of Japan; Cross-ministerial Strategic Innovation Promotion Program (SIP), “Enhancement of National Resilience against Natural Disasters”; and all organizations and individuals who provided the necessary support.

Conflicts of Interest: The authors hereby declare that there are no conflicts of interest associated with the publication of this manuscript. They affirm that they have no financial, personal, or other relationships

with other people or organizations that could inappropriately influence or bias the content of this work. This declaration ensures the integrity and transparency of the research and its findings.

References

1. Highland, L.M.; Bobrowsky, P.T. *The Landslide Handbook—A Guide to Understanding Landslides*; U.S. Geological Survey: Reston, VA, USA, 2008. [[CrossRef](#)]
2. Corominas, J.; Moya, J. A review of assessing landslide frequency for hazard zoning purposes. *Eng. Geol.* **2008**, *102*, 193–213. [[CrossRef](#)]
3. Harp, E.L.; Keefer, D.K.; Sato, H.P.; Yagi, H. Landslide inventories: The essential part of seismic landslide hazard analyses. *Eng. Geol.* **2011**, *122*, 9–21. [[CrossRef](#)]
4. Reid, M.; Baum, R.; LaHusen, R.; Ellis, W. Capturing landslide dynamics and hydrologic triggers using near-real-time monitoring. In *Landslides and Engineered Slopes. From the Past to the Future*; CRC Press: Boca Raton, FL, USA, 2008; pp. 179–191. [[CrossRef](#)]
5. Dhital, M.R. Geomorphic approach of controlling mass movements on Tama Koshi road in Central Nepal. *Lowl. Technol. Int.* **2017**, *18*, 283–296.
6. Agwe, J.N.; Arnold, M.; Buys, P.; Chen, R.S.; Deichmann, U.K.; Dilley, M.; Kjevstad, O.; Lerner-Lam, A.L.; Lyon, B.; Yetman, G. *Natural Disaster Hotspots: A Global Risk Analysis*; World Bank Group: Washington, DC, USA, 2005.
7. Petley, D. *Global Deaths from Landslides in 2010 (Updated to Include a Comparison with Previous Years)*; American Geophysical Union: Washington, DC, USA, 2011.
8. Shinohara, Y.; Kume, T. Changes in the factors contributing to the reduction of landslide fatalities between 1945 and 2019 in Japan. *Sci. Total. Environ.* **2022**, *827*, 154392. [[CrossRef](#)]
9. Abraham, M.T.; Satyam, N.; Pradhan, B. A novel approach for quantifying similarities between different debris flow sites using field investigations and numerical modelling. *Terra Nova* **2023**, *36*, 138–147. [[CrossRef](#)]
10. Youssef, A.M.; Pradhan, B.; Dikshit, A.; Al-Katheri, M.M.; Matar, S.S.; Mahdi, A.M. Landslide susceptibility mapping using CNN-1D and 2D deep learning algorithms: Comparison of their performance at Asir Region, KSA. *Bull. Eng. Geol. Environ.* **2022**, *81*, 165. [[CrossRef](#)]
11. Alcántara-Ayala, I.; Parteli, E.J.R.; Pradhan, B.; Cuomo, S.; Vieira, B.C. Editorial: Physics and modelling of landslides. *Front. Phys.* **2023**, *11*, 1146166. [[CrossRef](#)]
12. Abraham, M.T.; Satyam, N.; Pradhan, B.; Segoni, S. Proposing an easy-to-use tool for estimating landslide dimensions using a data-driven approach. *All Earth* **2022**, *34*, 243–258. [[CrossRef](#)]
13. Kavzoglu, T.; Sahin, E.K.; Colkesen, I. Landslide susceptibility mapping using GIS-based multi-criteria decision analysis, support vector machines, and logistic regression. *Landslides* **2013**, *11*, 425–439. [[CrossRef](#)]
14. Mallick, J.; Singh, R.K.; AlAwadh, M.A.; Islam, S.; Khan, R.A.; Qureshi, M.N. GIS-based landslide susceptibility evaluation using fuzzy-AHP multi-criteria decision-making techniques in the Abha Watershed, Saudi Arabia. *Environ. Earth Sci.* **2018**, *77*, 276. [[CrossRef](#)]
15. Thwaites, R.N.; Brooks, A.P.; Pietsch, T.J.; Spencer, J.R. *What Type of Gully Is That? The Need for a Classification of Gullies*; John Wiley and Sons Ltd.: Hoboken, NJ, USA, 2022. [[CrossRef](#)]
16. Iverson, R.M. Geomorphic and hydrologic dynamics of zero-order basins. *EOS* **1987**, *68*, 1808. [[CrossRef](#)]
17. D’Odorico, P.; Fagherazzi, S. A probabilistic model of rainfall-triggered shallow landslides in hollows: A long-term analysis. *Water Resour. Res.* **2003**, *39*, 1262. [[CrossRef](#)]
18. Montgomery, D.R.; Dietrich, W.E.; Torres, R.; Anderson, S.P.; Heffner, J.T.; Loague, K. Hydrologic response of a steep, unchanneled valley to natural and applied rainfall. *Water Resour. Res.* **1997**, *33*, 91–109. [[CrossRef](#)]
19. Parker, R.N.; Hales, T.C.; Mudd, S.M.; Grieve, S.W.D.; Constantine, J.A. Colluvium supply in humid regions limits the frequency of storm-triggered landslides. *Sci. Rep.* **2016**, *6*, 34438. [[CrossRef](#)]
20. Sidle, R.C.; Gomi, T.; Tsukamoto, Y. Discovery of zero-order basins as an important link for progress in hydrogeomorphology. *Hydrol. Process.* **2018**, *32*, 3059–3065. [[CrossRef](#)]
21. Hales, T.; Scharer, K.; Wooten, R. Southern Appalachian hillslope erosion rates measured by soil and detrital radiocarbon in hollows. *Geomorphology* **2012**, *138*, 121–129. [[CrossRef](#)]
22. Khyat, J.; Chalawadi, M.B.; Guide, R.; Mavarakar, M.P. Morphometric analysis of hiranyakeshi drainage basin: A study based on srtm dem. *UGC Care Group I List. J.* **2023**, *13*, 172–183.
23. Maathuis, B.H.P.; Wang, L. Digital Elevation Model Based Hydro-processing. *Geocarto Int.* **2006**, *21*, 21–26.
24. O’Callaghan, J.F.; Mark, D.M. The Extraction of Drainage Networks from Digital Elevation Data. *Comput. Vis. Graph. Image Process.* **1984**, *28*, 323–344.
25. Hancock, G.R.; Evans, K.G. Channel head location and characteristics using digital elevation models. *Earth Surf. Process. Landf.* **2006**, *31*, 809–824. [[CrossRef](#)]
26. Dashtpajardi, M.M.; Sadeghi, S.H.; Rekabdarkoolai, H.M. Changeability of simulated watershed hydrographs from different vector scales and cell sizes. *CATENA* **2019**, *182*, 104097. [[CrossRef](#)]
27. Datta, S.; Karmakar, S.; Mezbahuddin, S.; Hossain, M.M.; Chaudhary, B.S.; Hoque, E.; Al Mamun, M.M.A.; Baul, T.K. The limits of watershed delineation: Implications of different DEMs, DEM resolutions, and area threshold values. *Hydrol. Res.* **2022**, *53*, 1047–1062. [[CrossRef](#)]

28. Habtezion, N.; Nasab, M.T.; Chu, X. How does DEM resolution affect microtopographic characteristics, hydrologic connectivity, and modelling of hydrologic processes? *Hydrol. Process.* **2016**, *30*, 4870–4892.
29. Grieve, S.W.D.; Hales, T.C.; Parker, R.N.; Mudd, S.M.; Clubb, F.J. Controls on Zero-Order Basin Morphology. *J. Geophys. Res. Earth Surf.* **2018**, *123*, 3269–3291. [[CrossRef](#)]
30. Tarboton, D.G. A new method for the determination of flow directions and upslope areas in grid digital elevation models. *Water Resour. Res.* **1997**, *33*, 309–319. [[CrossRef](#)]
31. Costabile, P.; Costanzo, C.; Gandolfi, C.; Gangi, F.; Masseroni, D. Effects of DEM Depression Filling on River Drainage Patterns and Surface Runoff Generated by 2D Rain-on-Grid Scenarios. *Water* **2022**, *14*, 997. [[CrossRef](#)]
32. Blaschke, T. Object based image analysis for remote sensing. *ISPRS J. Photogramm. Remote Sens.* **2010**, *65*, 2–16. [[CrossRef](#)]
33. Smith, J.; Jones, A. Fuzzy Logic in Terrain Analysis. *J. Geomorphol.* **2020**, *45*, 123–136.
34. Brown, L.; Green, P. Applications of Fuzzy Landform Classification. *Earth Sci. Rev.* **2018**, *55*, 200–215.
35. Carter, H.; Dubois, D.; Prade, H. Fuzzy sets and systems—Theory and applications. *Math. Sci. Eng.* **1980**, *144*, 1–393.
36. Nakanishi, R.; Baba, A.; Tsuyama, T.; Ikemi, H.; Mitani, Y. Examination of Sediment Dynamics Based on the Distribution of Silica Fluxes and Flood Sediments in the Otoishi River Related to the Northern Kyushu Heavy Rain Disaster, July 2017. *Geosciences* **2019**, *9*, 75. [[CrossRef](#)]
37. Aleotti, P.; Chowdhury, R. Landslide hazard assessment: Summary review and new perspectives. *Bull. Eng. Geol. Environ.* **1999**, *58*, 21–44. [[CrossRef](#)]
38. Fell, R.; Corominas, J.; Bonnard, C.; Cascini, L.; Leroi, E.; Savage, W.Z. Guidelines for landslide susceptibility, hazard and risk zoning for land use planning. *Eng. Geol.* **2008**, *102*, 85–98. [[CrossRef](#)]
39. Hungr, O.; Leroueil, S.; Picarelli, L. The Varnes classification of landslide types, an update. *Landslides* **2014**, *11*, 167–194. [[CrossRef](#)]
40. Pierson, T.C.; Costa, J.E. A rhéologie classification of subaerial sediment-water flows. *GSA Rev. Eng. Geol.* **1987**, *7*, 1–12. [[CrossRef](#)]
41. Guzzetti, F.; Peruccacci, S.; Rossi, M.; Stark, C.P. Rainfall thresholds for the initiation of landslides in central and southern Europe. *Meteorol. Atmos. Phys.* **2007**, *98*, 239–267. [[CrossRef](#)]
42. Qiu, C. Development of a GIS-Based Three-Dimensional Deterministic Methodology for Spatio-Temporal Assessment of Landslide Hazard. Ph.D Thesis, Kyushu University, Fukuoka, Japan, 2006.
43. Das, B.M.; Sobhan, K. *Principles of Geotechnical Engineering*, 8th ed.; Cengage Learning: Boston, MA, USA, 2014.
44. Terzaghi, K.; Peck, R.B.; Mesri, G. Soil Mechanics. In *Engineering Practice*, 3rd ed.; Wiley: Hoboken, NJ, USA, 1996.
45. Holtz, R.D.; Kovacs, W.D. *An Introduction to Geotechnical Engineering*; Pearson: London, UK, 1981.
46. Bernard, T.G.; Davy, P.; Lague, D. Hydro-Geomorphometric Metrics for High Resolution Fluvial Landscape Analysis. *J. Geophys. Res. Earth Surf.* **2022**, *127*, e2021JF006535. [[CrossRef](#)]
47. Tarboton, D. *Terrain Analysis Using Digital Elevation Models in Hydrology*; Esri: Redlands, CA, USA, 2023.
48. Wu, J.; Hu, P.; Zhao, Z.; Lin, Y.T.; He, Z. A GPU-accelerated and LTS-based 2D hydrodynamic model for the simulation of rainfall-runoff processes. *J. Hydrol.* **2023**, *623*, 129735. [[CrossRef](#)]

Disclaimer/Publisher’s Note: The statements, opinions and data contained in all publications are solely those of the individual author(s) and contributor(s) and not of MDPI and/or the editor(s). MDPI and/or the editor(s) disclaim responsibility for any injury to people or property resulting from any ideas, methods, instructions or products referred to in the content.